OPTIMIZATION DESIGN OF CROSS-LAYER CABLE-BRACING INERTER SYSTEM FOR MULTI-MODAL SEISMIC VIBRATION

J. Kang [(1)], S. Xue [(2)], L. Xie [(3)], R. Zhang [(4)]
[(1)] *Master Candidate, Tongji University, Shanghai, China, kangjianfei@tongji.edu.cn*
[(2)] *Professor, Tongji University, Shanghai, China, xue@tongji.edu.cn*
[(3)] *Associate Professor, Tongji University, Shanghai, China, liyuxie@tongji.edu.cn*
[(4)] *Associate Professor, Tongji University, Shanghai, China, zhangruifu@tongji.edu.cn*

Abstract

In this paper, the influence of higher-order modes on seismic response of the high-rise structures is taken into consideration. Making full use of the cable-bracing inerter system (CIS) providing easy access to installment, which enables the inerter system attached to non-consecutive floors levels of the main structure be realized easily, a novel brace configuration scheme of inerter system is proposed, called cross-layer installed cable-bracing inerter system(CCIS), to reduce both first and higher modes vibrations. A unified motion equation of a structure equipped with CIS is proposed. The equivalent two-degree-of-freedom system of the multiple-degree-of-freedom (MDOF) structure equipped with CCIS is used to illustrate the mass ratio enhancement of the cross-layer installation.

A practical and applicable design approach, explicitly considering cost associated with control forces, is herein developed to identify the advantages of multiple CCISs with appropriate location distribution and optimal parameters. Considering the uncertainty of seismic ground motion, the seismic excitation is modeled as a stochastic stationary process, and the response statistics for linear structural systems are obtained through state-space analysis to meet the requirements of multiple iterations in optimization process. The objective function related to control forces is adopted as one of the two optimal objectives, whereas structural performance is incorporated in the design, representing different specific levels of vibration suppression be achieved through the inerter system implementation, as another. The proposed approach is illustrated using a 10-story benchmark structure. The optimum results and optimal parameters show that the same target performance, CCIS has obvious advantages in terms of minimizing the control force, and maintaining low damping, inerter mass requirements. The frequency-domain and time-domain analysis further demonstrates the high efficiency of CCIS for higher-order mode control and the advantages of CCIS over inter-layer installed inerter system (IIS) in seismic vibration control.

Keywords: cross-layer; cable-bracing inerter system; multi-modal

1 Introduction

Various energy dissipation devices and dampers have been developed in recent years to ensure the performance of structure vibration under seismic excitation. As the concept of inerter was formally proposed by Smith [1], inerter is increasingly used in seismic vibration control.

Inerter is an element, which can change its inner movement mechanism, such as translating linear motion to high-speed rotational motion, changing the liquid flow velocity, to obtain mass amplification effect. Inerter, used as a surrogate of the traditional mass, has numerous application forms, the most famous of which is the tuned viscous mass damper (TVMD) derived from the rotary damping system proposed firstly by Arakaki [2], which has been applied in practical structure [3]. Ikago et al. made a series of researches on the optimization of TVMD, from the fixed-point method [4] of single-degree-of-freedom (SDOF) with TVMD to the optimization of MDOF with TVMDs using SQP [5, 6] and its simpler design method [7]. As one of three commonly used mechanical layouts, the damping enhancement effect [8] and H_2 optimization [9, 10] of TVMD also have been studied by Pan et al.

Meanwhile, the research on the support system of inerter, focusing on practical applications has also developed in recent years. Sugimura et al.[3] studied the practical design of installing the inerter system in the structure using a V-shape steel brace combined with nature rubbers as tune spring. Xie et al. [11] studied SDOF with a CIS, showing the convenience and effectiveness of the cable-bracing method.

Considering the practical problems caused by the excessive inerter mass and damping requirements of using a single inerter system to control the vibration of MDOF structure and the excessive damper number requirement of using multiple IISs, in this paper, we propose multiple CCISs as an alternate. The advantages of cross-layer installation of inerter system have been demonstrated by Taflanidis et al. [12] using a commonly mechanical layout TMDI. However, caused by the limitation of TMDI, as a modification method of pendulum-like tuned mass damper, Taflanidis et al. only focused on the form of cross-layers installed at the top of the structure. In [13], Ogino and Sumiyama considered the design of a high-rise building using TVMD installed across three consecutive layers, which proved the practicality of the cross-layers installation method, while the location and distribution optimizations of the cross-layer installed inerter system is insufficient. In this paper, we focus on filling this gap. First, in Section 2, a unified motion equation of CIS equipped in the structure is established. An equivalent two-degree-of-freedom system is used to illustrate the mass ratio enhancement advantage of cross-layer installation. In Section 3, an extended state-space equation, considering the Kanai-Tajimi power spectrum, is formulated and an optimization method for CIS in the MDOF structure is proposed. In Section 4, applying the proposed optimization method to a 10-story benchmark model illustrates its effectiveness. By comparing the optimum results of CCIS and ICIS in the frequency domain and time history analysis, the advantages of CCIS are explained.

2 Cable-bracing inerter system

2.1 SDOF structure with the cable-bracing inerter system and its formulation

The cable-bracing inerter system consists of four parts: displacement transfer cable, soft spring for tuning, inerter, and energy dissipation element. The connection methods between the CIS and the main structure have been expanded due to the introduction of the cable. For simplicity, this article only discusses a direct installation scenario, as shown in Fig. 1.

The governing equation of motion of an SDOF with the CIS can be expressed as:

$$\begin{cases} m\ddot{u}+c\dot{u}+ku+2k_{\mathrm{d}}(u\cos\alpha-u_{\mathrm{d}})\cos\alpha=-m\ddot{u}_0 \\ m_{\mathrm{d}}\ddot{u}_{\mathrm{d}}+c_{\mathrm{d}}\dot{u}_{\mathrm{d}}+2k_{\mathrm{d}}(u_{\mathrm{d}}-u\cos\alpha)=0 \end{cases} \tag{1}$$

where, u and u_d are the displacement of the SDOF structure and the relative deformation of the inerter respectively; m, k, c are the mass, stiffness damping coefficient of the SDOF structure respectively; m_d, k_d, c_d are the inerter coefficient, tuned soft spring stiffness and damping coefficient of energy dissipation element; α is the installation angle of the cable.

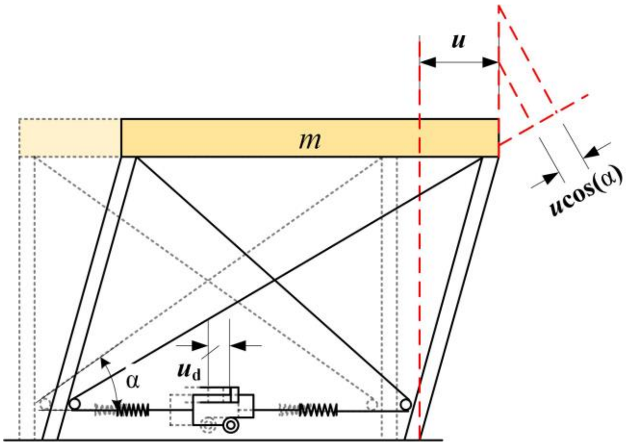

Fig. 1 Schematic of an SDOF structure with the CIS

To unify different installation forms, the installation efficiency coefficient β, defined by the displacement of the inerter system caused by the unit structure displacement, should be introduced. From the geometric relationship shown in Fig. 1, the installation efficiency coefficient β of the direct installation scenario equals to $\cos\alpha$. Defining the equivalent inerter displacement as $u_e = \frac{u_d}{\beta}$, as shown in Fig. 2, the Eq. (1) can be rearranged as:

$$\begin{cases} m\ddot{u} + c\dot{u} + ku + k_e(u - u_e) = -m\ddot{u}_0 \\ m_e\ddot{u}_e + c_e\dot{u}_e + k_e(u_e - u) = 0 \end{cases} \tag{2}$$

where, $m_e = m_d\beta^2$, $c_e = c_d\beta^2$, $k_e = 2k_d\beta^2$ are equivalent inerter coefficient, equivalent damping and equivalent stiffness respectively.

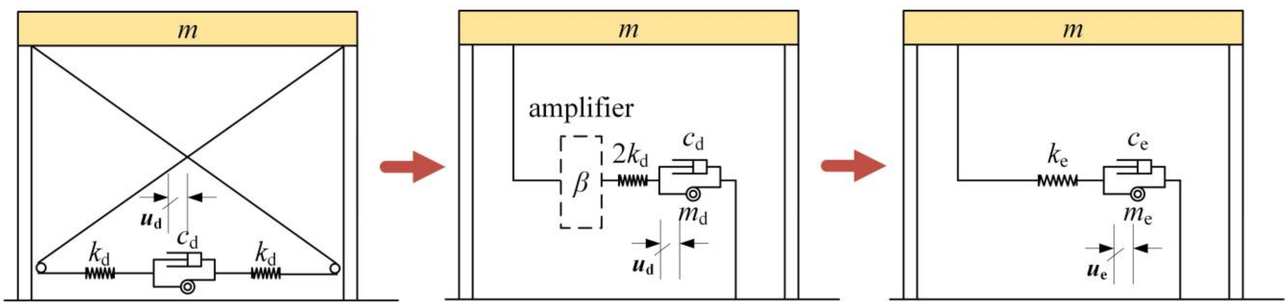

Fig. 2 Simplification process of direct installed CIS

2.2 MDOF structure with the cable-bracing inerter system and the mass ratio enhancement of the cross-layer installation

The governing equation of motion of an n-DOF without controlled is as follows:

$$\mathbf{M}_{\mathrm{p}}\ddot{x}_{\mathrm{p}} + \mathbf{C}_{\mathrm{p}}\dot{x}_{\mathrm{p}} + \mathrm{K}_{\mathrm{p}}x_{\mathrm{p}} = -\mathbf{M}_{\mathrm{p}}\mathbf{r}_{\mathrm{p}}\ddot{x}_{0} \tag{3}$$

where $x_{\mathrm{p}} = \{x_{\mathrm{p}1}, x_{\mathrm{p}2}, \ldots x_{\mathrm{pn}}\}^{T}$ is the displacement vector of the MDOF structure relative to the ground; $\mathbf{M}_{\mathrm{p}} = diag\{m_1, m_2, \ldots m_{\mathrm{n}}\}$, $\mathbf{K}_{\mathrm{p}} = \mathbf{T}^{T} diag(k_{\mathrm{p}1}, k_{\mathrm{p}2}, \ldots k_{\mathrm{pn}})\mathbf{T}$, $\mathbf{C}_{\mathrm{p}} = \mathbf{T}^{T} diag(c_{\mathrm{p}1}, c_{\mathrm{p}2}, \ldots c_{\mathrm{pn}})\mathbf{T}$ denote mass, stiffness and damping matrices of the primary structure respectively; $\mathbf{r}_{\mathrm{p}} = \{1,1,\ldots,1\}^{T}$ is the influence coefficient vector. $\mathbf{T}$ is an n-dimension square matrix with 1 in the diagonal and -1 in the first off-diagonal denoting a transformation matrix defining relative deformation between consecutive floors.

Similar to the SDOF structure, the n-DOF structure in which a CIS directly installed between the *r-th* and *s-th* layer (r<s) can be simplified to the model shown in Fig. 3. The motion equation is described as:

$$\mathbf{M}\ddot{x} + \mathbf{C}\dot{x} + \mathrm{K}x = -\mathbf{M}\mathbf{r}\ddot{x}_{0} \tag{4}$$

where $x = \{x_{\mathrm{p}}^{T}, u_{\mathrm{e}}\}^{T}$, $\mathbf{r} = \{\mathbf{r}_{\mathrm{p}}^{T}, 0\}^{T}$, $\mathbf{M} = \begin{bmatrix} \mathbf{M}_{\mathrm{p}} & \\ & m_{\mathrm{e}} \end{bmatrix}$, $\mathbf{C} = \begin{bmatrix} \mathbf{C}_{\mathrm{p}} & \\ & c_{\mathrm{e}} \end{bmatrix}$, $\mathbf{K} = \begin{bmatrix} \mathbf{K}_{\mathrm{p}} + r_{\mathrm{c}}k_{\mathrm{e}}r_{\mathrm{c}}^{T} & -k_{\mathrm{e}}r_{\mathrm{c}} \\ -r_{\mathrm{c}}^{T}k_{\mathrm{e}}^{T} & k_{\mathrm{e}} \end{bmatrix}$; r_{c} is an n-dimension vector, denoting the installation location of the CIS. Only the *r-th* and *s-th* entry of r_{c} are -1 and 1 respectively, and the remaining entries are all 0.

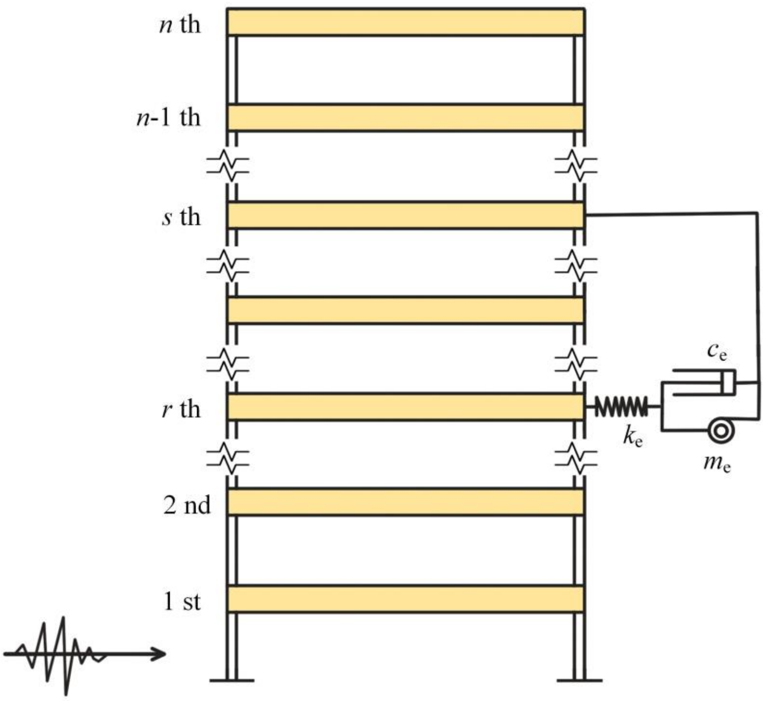

Fig. 3 Schematic of an MDOF structure with the CIS

Eq. (4) is a general equation, which can express different types of CIS connection methods by changing parameters($s - r = 1$ denotes the ICIS, $s - r > 1$ denotes the CCIS). At the same time, $u_{\mathrm{e}}, m_{\mathrm{e}}, c_{\mathrm{e}}, k_{\mathrm{e}}, r_{\mathrm{c}}$ can be expanding into suitable matrixes to denote the situation of multiple CIS installed in the structure, which will be used in section 3.

Previous studies [14] have shown that the vibration modes of the structure with TVMD distributed proportional to the structural stiffness is almost the same with those of uncontrolled structure. To analyze the mass ratio enhancement of the cross-layer installation through an equivalent two-degree-of-freedom system, it is assumed that the n-DOF structure equipped with a CIS vibrates approximately in an uncontrolled mode ${}_i\phi$. The displacement vector of the primary structure x_p and the equivalent inerter displacement u_e be represented by modal coordinate ${}_i\alpha_\mathrm{p}$ and ${}_i\alpha_\mathrm{d}$ respectively as follows:

$$\begin{cases} x_\mathrm{p} = {}_i\alpha_{\mathrm{p}\,i}\phi \\ u_\mathrm{e} = {}_i\alpha_\mathrm{d} r_\mathrm{c}{}^T{}_i\phi \end{cases} \tag{5}$$

Therefore, the kinetic energy E_T ,strain energy E_U and dissipated energy E_D of the MDOF structure with the CCIS can be expressed by the following equation:

$$\begin{cases} E_\mathrm{T} = \frac{1}{2}{}_i\dot{\alpha}_\mathrm{p}^2\,{}_i\phi^T\mathbf{M}_{\mathrm{p}i}\phi + \frac{1}{2}{}_i\dot{\alpha}_\mathrm{d}^2\,{}_i\phi^T r_\mathrm{c} m_\mathrm{e} r_\mathrm{c}{}^T{}_i\phi \\ E_\mathrm{U} = \frac{1}{2}{}_i\alpha_\mathrm{p}^2\,{}_i\phi^T\mathbf{K}_{\mathrm{p}i}\phi + \frac{1}{2}({}_i\alpha_\mathrm{p} - {}_i\alpha_\mathrm{d})^2\,{}_i\phi^T r_\mathrm{c} k_\mathrm{e} r_\mathrm{c}{}^T{}_i\phi \\ E_\mathrm{D} = \frac{1}{2}{}_i\dot{\alpha}_\mathrm{p}^2\,{}_i\phi^T\mathbf{C}_{\mathrm{p}i}\phi + \frac{1}{2}{}_i\dot{\alpha}_\mathrm{d}^2\,{}_i\phi^T r_\mathrm{c} c_\mathrm{e} r_\mathrm{c}{}^T{}_i\phi \end{cases} \tag{6}$$

Assuming $L = E_\mathrm{T} - E_\mathrm{U}$,the Euler-Lagrange equation of the MDOF structure with the CIS as follow:

$$\begin{cases} \frac{d}{dt}\left(\frac{\partial}{\partial\,{}_i\dot{\alpha}_\mathrm{p}}L\right) - \frac{\partial}{\partial\,{}_i\alpha_\mathrm{p}}L + \frac{\partial}{\partial\,{}_i\dot{\alpha}_\mathrm{p}}E_\mathrm{D} = 0 \\ \frac{d}{dt}\left(\frac{\partial}{\partial\,{}_i\dot{\alpha}_\mathrm{d}}L\right) - \frac{\partial}{\partial\,{}_i\alpha_\mathrm{d}}L + \frac{\partial}{\partial\,{}_i\dot{\alpha}_\mathrm{d}}E_\mathrm{D} = 0 \end{cases} \tag{7}$$

Substituting Eq. (6) into Eq. (7) gives the following equation.

$$\begin{cases} {}_i\phi^T\mathbf{M}_{\mathrm{p}i}\phi\cdot{}_i\ddot{\alpha}_\mathrm{p} + {}_i\phi^T\mathbf{C}_{\mathrm{p}i}\phi\cdot{}_i\dot{\alpha}_\mathrm{p} + {}_i\phi^T\mathbf{K}_{\mathrm{p}i}\phi\cdot{}_i\alpha_\mathrm{p} + {}_i\phi^T r_\mathrm{c} k_\mathrm{e} r_\mathrm{c}{}^T{}_i\phi\cdot({}_i\alpha_\mathrm{p} - {}_i\alpha_\mathrm{d}) = 0 \\ {}_i\phi^T r_\mathrm{c} m_\mathrm{e} r_\mathrm{c}{}^T{}_i\phi\cdot{}_i\ddot{\alpha}_\mathrm{d} + {}_i\phi^T r_\mathrm{c} c_\mathrm{e} r_\mathrm{c}{}^T{}_i\phi\cdot{}_i\dot{\alpha}_\mathrm{d} + {}_i\phi^T r_\mathrm{c} k_\mathrm{e} r_\mathrm{c}{}^T{}_i\phi\cdot({}_i\alpha_\mathrm{d} - {}_i\alpha_\mathrm{p}) = 0 \end{cases} \tag{8}$$

Compared Eq. (8) with Eq. (2), the generalized mass, generalized damping coefficient and generalized stiffness of the CIS can be expressed as:

$$\begin{cases} M_\mathrm{d} = {}_i\phi^T r_\mathrm{c} m_\mathrm{e} r_\mathrm{c}{}^T{}_i\phi \\ C_\mathrm{d} = {}_i\phi^T r_\mathrm{c} c_\mathrm{e} r_\mathrm{c}{}^T{}_i\phi \\ K_\mathrm{d} = {}_i\phi^T r_\mathrm{c} k_\mathrm{e} r_\mathrm{c}{}^T{}_i\phi \end{cases} \tag{9}$$

According to Eq. (9), when the CIS is installed cross layers, the vector r_c , denoting the installation location of the CIS, causes the model displacement between the r and s layers to be superimposed, thereby bring about mass ratio enhancement.

3 Optimum Seismic Control of a MDOF system with CIS

3.1 Evaluation of Seismic Response

Considering the uncertainty of seismic ground motion, instead of using any particular recorded seismic motion, the seismic input action is simulated as a Kanai-Tajimi power spectrum:

$$S_{\mathrm{g}}(\omega)=\frac{\omega_{\mathrm{g}}^{4}+4\zeta_{\mathrm{g}}^{2}\omega^{2}\omega_{\mathrm{g}}^{2}}{(\omega_{\mathrm{g}}^{2}-\omega^{2})^{2}+4\zeta_{\mathrm{g}}^{2}\omega^{2}\omega_{\mathrm{g}}^{2}}S_{0} \tag{10}$$

where, ω_{g} , ζ_{g} are frequency and damping coefficient, respectively, of the SDOF, used to represent the supporting ground properties. S_0 is the intensity of the white noise excitation at the bedrock.

During the optimization process, iterative evaluation of the seismic response is required. Therefore, the state-space approach, which is efficient at calculating the seismic response, is employed. Extend Eq. (4) into the motion equation of a MDOF structure with t CISs and rewrite it into a state-space equation as:

$$\dot{x}_{\mathrm{R}}=\mathbf{A}_{\mathrm{R}}x_{\mathrm{R}}+\mathbf{E}_{\mathrm{R}}w \tag{11}$$

where, $x_{\mathrm{R}}=\left\{x_{\mathrm{p}}^{T} \quad x_{\mathrm{e}}^{T} \quad \dot{x}_{\mathrm{p}}^{T} \quad \dot{x}_{\mathrm{e}}^{T}\right\}^{T}$, $\mathbf{A}_{\mathrm{R}}=\begin{bmatrix}0_{(n+t)\times(n+t)} & \mathbf{I}_{(n+t)\times(n+t)}\\ -\mathbf{M}_{\mathrm{R}}^{-1}\mathbf{K}_{\mathrm{R}} & -\mathbf{M}_{\mathrm{R}}^{-1}\mathbf{C}_{\mathrm{R}}\end{bmatrix}$, $\mathbf{E}_{\mathrm{R}}=\begin{bmatrix}0_{1\times(n+t)} & -\mathbf{r}_{\mathrm{p}}^{T} & 0_{1\times t}\end{bmatrix}^{T}$;w denotes the white noise input and $\mathbf{M}_{\mathrm{R}}=\begin{bmatrix}\mathbf{M}_{\mathrm{p}} & \\ & \mathbf{M}_{\mathrm{e}}\end{bmatrix}$, $\mathbf{C}=\begin{bmatrix}\mathbf{C}_{\mathrm{p}} & \\ & \mathbf{C}_{\mathrm{e}}\end{bmatrix}$, $\mathbf{K}=\begin{bmatrix}\mathbf{K}_{\mathrm{p}}+\mathbf{R}_{\mathrm{c}}\mathbf{K}_{\mathrm{e}}\mathbf{R}_{\mathrm{c}}^{T} & -\mathbf{K}_{\mathrm{e}}\mathbf{R}_{\mathrm{c}}\\ -\mathbf{R}_{\mathrm{c}}^{T}\mathbf{K}_{\mathrm{e}}^{T} & \mathbf{K}_{\mathrm{e}}\end{bmatrix}$; x_{e} , $\mathbf{M}_{\mathrm{e}}$, $\mathbf{C}_{\mathrm{e}}$, $\mathbf{K}_{\mathrm{e}}$, $\mathbf{R}_{\mathrm{c}}$ are expanded equivalent inerter coefficient matrix, equivalent damping matrix and equivalent stiffness matrix and the CIS location matrix respectively.

Rewrite the Kanai-Tajimi power spectrum Eq. (10) into the form of state-space equation:

$$\begin{cases}\dot{x}_{\mathrm{q}}=\mathbf{A}_{\mathrm{q}}x_{\mathrm{q}}+\mathbf{E}_{\mathrm{q}}w\\ \ddot{x}_{\mathrm{g}}=\mathbf{C}_{\mathrm{q}}x_{\mathrm{q}}\end{cases} \tag{12}$$

where, $\mathbf{A}_{\mathrm{q}}=\begin{bmatrix}0 & 1\\ -\omega_{\mathrm{g}}^{2} & -2\zeta_{\mathrm{g}}\omega_{\mathrm{g}}\end{bmatrix}$, $\mathbf{C}_{\mathrm{q}}=\sqrt{2\pi S_{0}}\begin{bmatrix}-\omega_{\mathrm{g}}^{2} & -2\zeta_{\mathrm{g}}\omega_{\mathrm{g}}\end{bmatrix}$, $\mathbf{E}_{\mathrm{q}}=\begin{bmatrix}0\\1\end{bmatrix}$

Combining Eq. (11) and Eq. (12), an extended state-space equation considering Kanai-Tajimi power spectrum excitation can be obtained:

$$\begin{cases}\dot{x}_{\mathrm{s}}=\mathbf{A}_{\mathrm{s}}x_{\mathrm{s}}+\mathbf{E}_{\mathrm{s}}w\\ z=\mathbf{C}_{\mathrm{s}}x_{\mathrm{s}}\end{cases} \tag{13}$$

where $x_{\mathrm{s}}=\begin{Bmatrix}x_{\mathrm{R}}\\ x_{\mathrm{q}}\end{Bmatrix}$, $\mathbf{A}_{\mathrm{s}}=\begin{bmatrix}\mathbf{A}_{\mathrm{R}} & \mathbf{E}_{\mathrm{R}}\mathbf{C}_{\mathrm{q}}\\ 0_{2\times(2n+2t)} & \mathbf{A}_{\mathrm{q}}\end{bmatrix}$, $\mathbf{E}_{\mathrm{s}}=\begin{bmatrix}0_{(2n+2t)\times1}\\ \mathbf{E}_{\mathrm{q}}\end{bmatrix}$. The output matrix $\mathbf{C}_{\mathrm{s}}$, used to calculate the performance vector z that includes inter-story drifts and forces of CISs , is $\begin{bmatrix}\mathbf{T} & & 0_{n\times(2n+2t+2)}\\ -\mathbf{R}_{\mathrm{c}}^{T}\mathbf{K}_{\mathrm{e}}^{T} & \mathbf{K}_{\mathrm{e}} & 0_{t\times(n+t+2)}\end{bmatrix}$.

According to the extended state-space Eq. (13), the covariance matrix of the output vector z is:

$$\mathbf{K}_{zz}=\mathbf{C}_{\mathrm{s}}\mathbf{P}\mathbf{C}_{\mathrm{s}}^{T} \tag{14}$$

where, the state covariance matrix P can be obtained by solving the Lyapunov equation, which can be easily done with the 'lypa' function in MATLAB:

$$\mathbf{A}_{\mathrm{s}}\mathbf{P}+\mathbf{P}\mathbf{A}_{\mathrm{s}}^{T}+\mathbf{E}_{\mathrm{s}}\mathbf{E}_{\mathrm{s}}^{T}=0 \tag{15}$$

3.2 Formulation of the Optimum Design Problem

The design of the CISs used to control the MDOF structure seismic response, includes layout design and parameters optimization design. Based on the uncontrolled relative modal deformation between the structural layers, the layout design can be predetermined. The parameters of each CIS need to be obtained through optimization, considering the seismic building performance and the CIS cost comprehensively.

The first objective J_{p}, representing the engineering demand, is defined by the sum of the CISs equipped structure story drifts, normalized by uncontrolled structure ones, with the same weight:

$$J_{\mathrm{p}} = \frac{1}{n}\sum_{i=1}^{n}\frac{\sigma_{\mathrm{z}}^{\mathrm{d}}(i)}{\sigma_{\mathrm{z0}}^{\mathrm{d}}(i)} \tag{16}$$

where, $\sigma_{\mathrm{z}}^{\mathrm{d}}(i)$, $\sigma_{\mathrm{z0}}^{\mathrm{d}}(i)$ denote the CISs equipped structure and the uncontrolled structure *i-th* story drift variance respectively.

The second objective $J_{\mathrm{F_d}}$, representing the CIS cost, is defined by the maximum force of those CISs equipped in the structure:

$$J_{\mathrm{F_d}} = \max_{i=1}^{t}\left\{\sigma_{\mathrm{F_d}}(i)\right\} \tag{17}$$

where, $\sigma_{\mathrm{F_d}}(i)$ denotes the *i-th* CIS control force response variance.

Although the increase of connection stiffness can achieve better control effect, it comes at the cost of tuning effects, which tremendously increase damping and quality requirements. To maximize the tuning effect of the CIS, the frequency of the CIS should be tuned to a certain mode, as Ikago et al. did in [5]:

$$_j\omega_r = \frac{1}{\sqrt{1-{}_j\mu}}\,{}_j\omega_0 \tag{18}$$

where, $_j\omega_r$, $_j\omega_0$ denote the frequency of CIS and uncontrolled structure respectively, and the left subscript j denotes the *j-th* mode. The *j-th* modal effective mass ratio $_j\mu$ is defined as follows:

$$_j\mu = \frac{{}_j\phi^T\,{}_j\mathbf{R}_{\mathrm{c}}\,{}_j\mathbf{M}_{\mathrm{e}}\,{}_j\mathbf{R}_{\mathrm{c}}^T\,{}_j\phi}{{}_j\phi^T\mathbf{M}_{\mathrm{p}}\,{}_j\phi} \tag{19}$$

where, $_j\mathbf{M}_{\mathrm{e}}$, $_j\mathbf{R}_{\mathrm{c}}$ donate the equivalent inerter coefficient matrix and location matrix of those CISs tuned to the *j-th* mode respectively.

Thus, the optimum design problem for CIS for the control of multi-modal seismic vibration is formulated as follows:

$$\begin{aligned}
&\text{find} && y=\left\{M_{\mathrm{e1}},M_{\mathrm{e2}},\ldots,M_{\mathrm{e}t},{}_1\omega_r,{}_2\omega_r,\ldots,{}_j\omega_r,{}_1\zeta_r,{}_2\zeta_r,\ldots,{}_j\zeta_r\right\}\\
&\text{to minimize} && J_{\mathrm{F_d}}(y)\\
&\text{subject to} && \begin{cases} J_{\mathrm{p}}(y)\le J_{\mathrm{target}}\\ {}_1\omega_r=\dfrac{1}{\sqrt{1-{}_1\mu}}\,{}_1\omega_0,\ {}_2\omega_r=\dfrac{1}{\sqrt{1-{}_2\mu}}\,{}_2\omega_0,\ldots,{}_1\omega_r=\dfrac{1}{\sqrt{1-{}_1\mu}}\,{}_1\omega_0\end{cases}
\end{aligned}$$

where, t, j denote the number of types of CIS installed in the structure and controlled modes of the structure. J_{target} is the target engineering demand limitation determined initial analysis of primary structure.

4 Design Example

4.1 Analysis Model

The benchmark structure used in this study is a 10-story building proposed by the JSSI [15], the detail information of which is shown in Table 1 and Fig.4

Table 1 Characteristics of the benchmark building

Story	**Mass m_i ($\times 10^3$kg)**	**Stiffness k_i ($\times 10^3$N/m)**	**Height(m)**
10	875.4	158550	4
9	649.5	180110	4
8	656.2	220250	4
7	660.2	244790	4
6	667.2	291890	4
5	670.1	306160	4
4	675.7	328260	4
3	680.0	383020	4
2	681.6	383550	4
1	699.9	279960	6

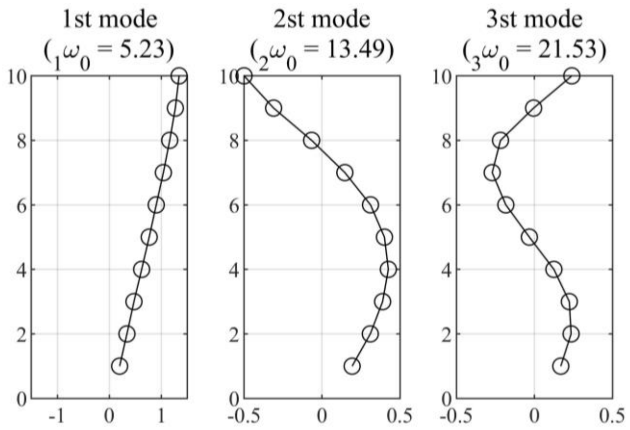

Fig. 4 participation mode vector of the uncontrolled benchmark building

4.2 Details for design optimization

In this model, it is assumed that three kinds of inerter are used, which is limited by practical applications. As is shown in Fig. 5, two layouts of CIS (CASE A, CASE B) are determined on the principle of modal relative displacement maximization. For CASE A, the ICIS of the upper four layers are tuned to the second mode, while other ICISs are tuned to the first mode. For CASE B, the CCIS crossing the top three layers is tuned to the second mode, while others are tuned to the first mode.

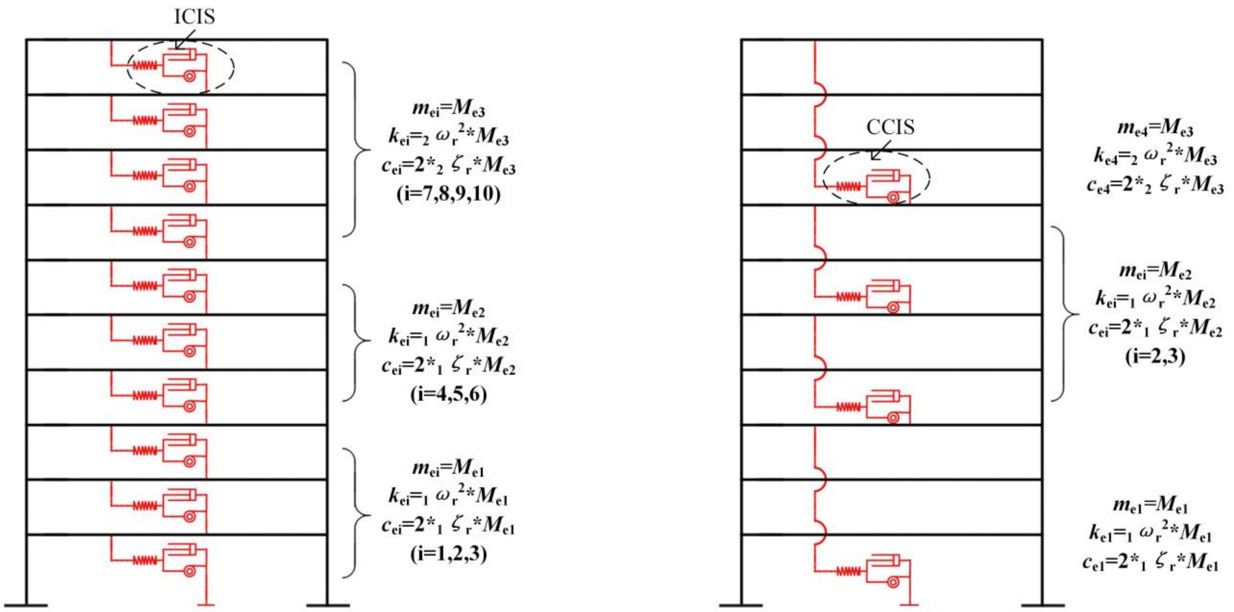

Fig. 5 Schematic of the benchmark building with CISs (a) CASE A (b) CASE B

In this study, the parameters ω_g , ζ_g , S_0 of the Kanai-Tajimi power spectrum are taken to have values $\omega_g = 4\pi$, $\zeta_g = 0.6$ and $S_0 = 0.0156\mathrm{m}^2 \cdot \mathrm{s}^{-3}$ .The initial analysis and iterative calculation of the primary structure show that the J_{target} can be selected as 0.5.

4.3 Results and discussion

Table 2 shows the optimum design parameters and two optimized objectives of CASE A and CASE B. It shows that under the same performance objective J_p, the maximum control force J_{F_d} in CASE B, which uses the CCISs, is reduced by about 7% compared with the ICISs used in CASE A, proving the advantage of CCIS in reducing control forces. From the perspective of parameter requirements, the maximum reduction in additional inerter and damper required by CCISs used in CASE B compared to ICISs in CASE A is 63.3% and 59.0% respectively, verifying the mass ratio enhancement of the cross-layer installation.

Table 2 Optimum designs

	CASE A	**CASE B**
M_{e1}	1.87×10^6 kg	0.79×10^6 kg
M_{e2}	2.53×10^6 kg	1.29×10^6 kg
M_{e3}	1.07×10^6 kg	0.39×10^6 kg
${}_1\omega_r$	3.21	3.23

${}_2\omega_r$	9.44	9.32
${}_1\zeta_r$	0.26	0.31
${}_2\zeta_r$	0.60	0.67
J_p	0.50	0.50
$J_{\mathrm{F_d}}$	7.67×10^5	7.14×10^5

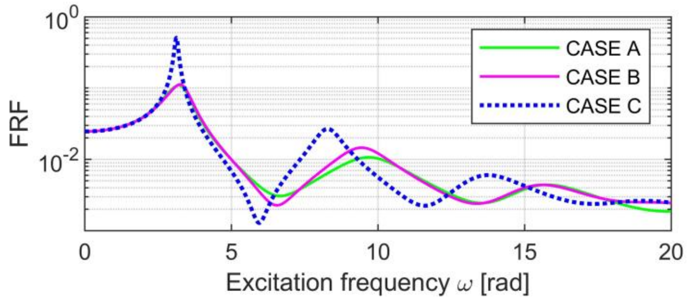

Fig. 6 frequency response functions (FRFs) of CASE A, CASE B and CASE C (the uncontrolled building)

The frequency response functions of CASE A and CASE B show that, as is shown in Fig. 6, both of them have similar excellent control effects on the first and second modes.

An artificial earthquake BCJ-L2 is employed as the input ground motion for time history analysis to further study the control effect of CASE A and CASE B. The analysis results, shown in Fig. 7, illustrate that the responses of the MDOF structure equipped with optimum CISs, regardless of CASE A or CASE B, is greatly reduced compared to the uncontrolled structure, which is shown in the figure as CASE C, and the story drifts generally does not exceed the limit of 0.01 with engineering accuracy. The damper forces, shown in Fig. 8, illustrates that the cross-layer installation can reduce the maximum control force, which is consistent with the analysis of the control force objective $J_{\mathrm{F_d}}$.

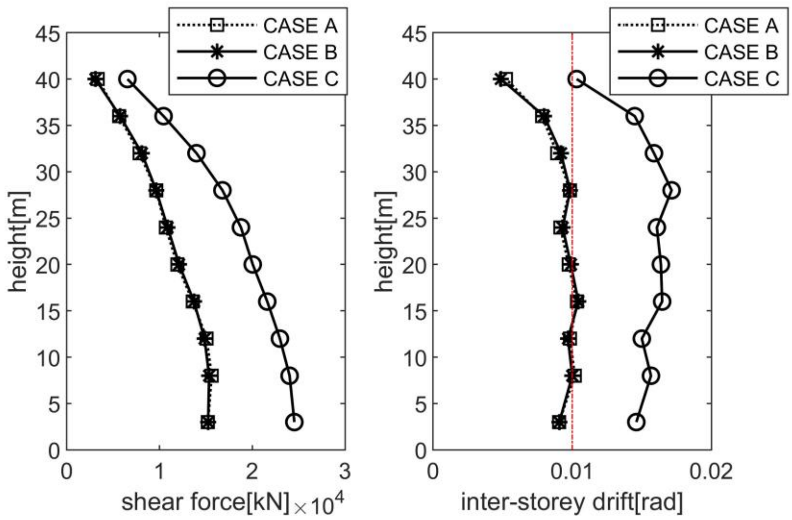

Fig. 7 Seismic responses (BCJ-L2) for CASE A, CASE B and CASE C (the uncontrolled building)

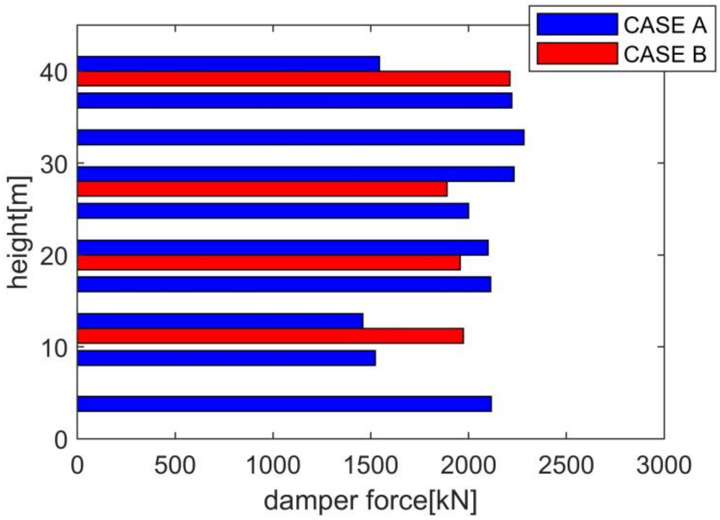

Fig. 8 Control forces in the CISs of CASE A, CASE B

5 Conclusions

In this paper, the authors present the multi-mode optimum designs for a MDOF structure equipped with ICIS and CCIS. The contributions of this study are as follows:

1. The installation efficiency coefficient β, which unifies the CIS with different installation forms, is proposed.
2. The equivalent two-degree-of-freedom system is used to prove the mass ratio enhancement effect of the cross-layer installation.
3. By constructing a reasonable state-space equation, a fast calculation method of seismic response considering a Kanai-Tajimi power spectrum input is established. The optimization problem of a MDOF structure equipped with CISs is transformed into a single-objective optimization problem with constraints by defining performance objective and cost objective.
4. A 10-story benchmark structure is taken as a design example, illustrating that the CCIS not only can reduce the control force but the requirements of additional inerter and damper. The seismic responses given by CCISs and ICISs are almost identical, verified in the paper through frequency domain and time domain analysis.

6 Acknowledgements

This study was supported by the National Natural Science Foundation of China (Grant No.51478356, No.51778490), the Key Program for International S&T Cooperation Projects of China (Grant No. 2016YFE0127600) and Open Research Fund Program of Guangdong Key Laboratory of Earthquake Engineering and Application Technology (Grant No. 2017B030314068).

7 References

[1] Smith MC. (2002): Synthesis of mechanical networks: the inerter. *41st IEEE Conference on Decision and Control*.

[2] Arakaki T, Kuroda H, Arima F (1999): Development of seismic devices applied to ball screw: Part 1 Basic performance test of RD-series. *Journal of Architecture and Building Science*, **5**(8), 239-244. (in Japanese)

[3] Sugimura Y, Goto W, Tanizawa H, Satio K, Ninomiya T, Nagasaku T (2012): Response control effect of steel building structure using tuned viscous mass damper. *Proceedings of the 15th World Conference on Earthquake Engineering.*

[4] Ikago K, Saito K, Inoue N (2012): Seismic control of single-degree-of-freedom structure using tuned viscous mass damper. *Earthquake Engineering & Structural Dynamics*, **41**(3), 453-474.

[5] Ikago K, Sugimura Y, Saito K, Inoue N (2010): Optimum seismic response control of multiple degree of freedom structures using tuned viscous mass dampers. *Proceedings of the Tenth International Conference on Computational Structures Technology.*

[6] Ikago K, Saito K, Inoue N (2011): Optimum multi-modal seismic control design of high-rise buildings using tuned viscous mass dampers. *Proceedings of the 13th International Conference on Civil, Structural and Environmental Engineering Computing, Chania, Crete, Greece.*

[7] Ikago K, Sugimura Y, Saito K, Inoue N (2012): Simple design method for a tuned viscous mass damper seismic control system. *Proceedings of the 15th World Conference on Earthquake Engineering, Lisbon, Portugal*.

[8] Zhang R, Zhao Z, Pan C, Ikago K, Xue S (2020): Damping enhancement principle of inerter system. *Structural Control and Health Monitoring*.e2523

[9] Pan C, Zhang R (2018): Design of structure with inerter system based on stochastic response mitigation ratio. *Structural Control and Health Monitoring*, **25**(6), e2169.

[10] Pan C, Zhang R, Luo H, Li C, Shen H (2018): Demand-based optimal design of oscillator with parallel-layout viscous inerter damper. *Structural Control and Health Monitoring*, **25**(1), e2051.

[11] Xie L, Ban X, Xue S, Ikago K, Kang J, Tang H (2019): Theoretical Study on a Cable-Bracing Inerter System for Seismic Mitigation. *Applied Sciences*,**9**(19), 4096.

[12] Taflanidis AA, Giaralis A, Patsialis D (2019): Multi-objective optimal design of inerter-based vibration absorbers for earthquake protection of multi-storey building structures. *Journal of the Franklin Institute*, **336**(14), 7754-7784.

[13] Ogino M, Sumiyama T (2014): Structural design of a high-rise building using tuned viscous mass dampers installed across three consecutive sotreys. *Twelveth International Conference on Computational Structures Technology, Naples, Italy*.

[14] Ikago K, Sugimura Y, Saito K, Inoue N (2018) Modal Response Characteristics of a Multiple-Degree-Of-Freedom Structure Incorporated with Tuned Viscous Mass Dampers. *Journal of Asian Architecture and Building Engineering*, **11**(2), 375-382.

[15] The Japan Society for Seismic Isolation (2005): *Manual for Design and Fabrication for Passive Vibration Control of Structures,* 2nd edition. (in Japanese)

